Journal of *Xenobiotics*

MDPI

Article

Microplastics and Nitrite Stress Affect Physiological and Metabolic Functions of the Hepatopancreas in Marine Shrimp

Yi-Fu Xing [1,2,†], Xuan-Yi Zhu [1,2,†], Hong-Biao Dong [1,2,3], Jian-Hua Huang [4], Ya-Fei Duan [1,2,3,*] and Jia-Song Zhang [1,2,3,*]

[1] South China Sea Fisheries Research Institute, Chinese Academy of Fishery Sciences, Guangzhou 510300, China
[2] Key Laboratory of South China Sea Fishery Resources Exploitation & Utilization, Ministry of Agriculture and Rural Affairs, Guangzhou 510300, China
[3] Key Laboratory of Efficient Utilization and Processing of Marine Fishery Resources of Hainan Province, Sanya Tropical Fisheries Research Institute, Sanya 572018, China
[4] Shenzhen Base of South China Sea Fisheries Research Institute, Chinese Academy of Fishery Sciences, Shenzhen 518121, China
* Correspondence: duanyafei89@163.com (Y.-F.D.); jiasongzhang@hotmail.com (J.-S.Z.)
† These authors contributed equally to this work.

Abstract

Nitrite is a common toxic substance in aquaculture, and microplastics are environmental pollutants capable of adsorbing small molecules/particles. Shrimp rely mainly on the hepatopancreas to accomplish detoxification metabolism. In this study, we investigated the individual and combined effects of nitrite and microplastics on the physiological function of the *P. vannamei* hepatopancreas. The results demonstrated that both nitrite and microplastics induced morphological damage, with the combined stress exacerbating tissue damage. Oxidative stress biochemical indicators were disrupted, and most enzyme activities and gene expression levels were upregulated to varying degrees in each experimental group. The expression levels of immune genes (*cytC*, *CASP-3*, *Crus*, *ALF*, and *proPO*), detoxification metabolism genes (*CYP450*, *EH1*, *SULT*, and *UGT*), and oxidative-stress-related genes (*ROMO1*, *SOD*, *GPx*, and *Trx*) exhibited different fluctuations. Nitrite and microplastic stress resulted in altered hepatopancreatic function, mainly involving amino acid biosynthesis and metabolism, ABC transporters, oxidative phosphorylation, and the mTOR pathway. We identified 17 metabolic biomarkers, including 6 lipids (Oleic acid, Prostaglandin G2, Linoleic acid, Palmitic acid, Docosahexaenoic acid, Docosapentaenoic acid), 6 amino acids (L-Leucine, Agmatine, L-Arginine, L-Tyrosine, Ornithine, N-Acetylornithine), and 5 carbohydrates (Glyceric acid, Citric acid, D-Mannose, Sorbitol, Fumaric acid). These findings suggest that nitrite and microplastic stresses cause hepatopancreatic tissue damage and induce oxidative stress, physiological and metabolic dysfunction in the shrimp *P. vannamei*, thereby impacting its normal physiological functions.

Keywords: marine shrimp; hepatopancreas; nitrite; microplastics; metabolism

Check for updates

Academic Editor: Stefano Magni

Received: 27 November 2025
Revised: 22 January 2026
Accepted: 23 January 2026
Published: 27 January 2026

Copyright: © 2026 by the authors. Licensee MDPI, Basel, Switzerland. This article is an open access article distributed under the terms and conditions of the Creative Commons Attribution (CC BY) license.

1. Introduction

The intensive high-density culture of Pacific white shrimp (*Penaeus vannamei*) often leads to frequent disease outbreaks due to environmental stress, significantly compromising the economic viability of the industry [1,2]. Nitrite is a critical limiting environmental stressor in shrimp aquaculture systems. The accumulation of residual feed and feces disrupts the nitrogen cycle in water [3], while the proliferation rate of nitrifying bacteria lags significantly behind the decomposition rate of organic matter, resulting in nitrite accumulation.

In scenarios of pond ecosystem imbalance or failed water quality management, nitrite concentrations can rise to 9 mg·L^{-1} and even 20 mg·L^{-1}, far exceeding levels found in natural environments (<0.046 mg·L^{-1}) and posing a lethal threat to shrimp survival and growth [4]. Concurrently, the extensive use of plastic products in aquaculture has led to microplastics, derived from their degradation, emerging as a novel class of environmental pollutants [5,6]. Microplastics have now been detected in rivers, aquaculture waters, and even within farmed aquatic organisms. Given the omnivorous diet of shrimp and the similarity in size between microplastics and shrimp feed particles, microplastics are readily ingested and enriched in shrimp, adversely affecting their health status [7].

The toxic effects of these individual pollutants on aquatic animals have been extensively documented [8]. The primary hazard of nitrite lies in its disruption of osmotic regulation, hemolymph oxygen-carrying capacity, and metabolic homeostasis in crustaceans, which can lead to mass mortality under severe conditions [9]. Exposure to nitrite at a concentration as low as 0.579 mmol·L^{-1} can induce metabolic disorders and reactive oxygen species (ROS) bursts in granulosa cells of *P. vannamei* [8]. Microplastics not only accumulate in the hepatopancreas but also cause direct damage to intestinal and gill tissues, reduce oxygen uptake efficiency, and induce oxidative stress [10–12]. Furthermore, their porous structure enables the adsorption of co-existing pollutants like nitrite, potentially leading to synergistic toxicity [13–15]. However, research on the combined effects of these two stressors on *P. vannamei* remains limited.

The hepatopancreas serves as a central organ integrating digestion, metabolism, and immune function in *P. vannamei*. Its epithelial cells are rich in metabolic enzymes and immune-related proteins, endowing it with potent detoxification and homeostatic regulation capacities, making it a sensitive target for environmental pollutants [16,17]. Previous studies have confirmed that nitrite can disrupt amino acid metabolism in the hepatopancreas, affecting energy supply and inducing immune responses and apoptosis [18–20]. Microplastics can induce oxidative stress, impair metabolic and detoxification functions, and cause significant pathological damage in the hepatopancreas [13,14]. Nevertheless, the histopathological characteristics, oxidative stress response patterns, regulatory mechanisms of key functional gene expression, and shifts in metabolic profiles under combined nitrite and microplastic stress remain unclear. Current research predominantly focuses on the effects of individual pollutants, lacking a systematic investigation into the synergistic interactions of multiple pollutants in aquaculture environments. This gap hinders a comprehensive understanding of the stress-induced damage mechanisms in real-world farming scenarios.

Therefore, this study systematically evaluates the individual and combined effects of nitrite and microplastic stress on the hepatopancreas of *P. vannamei*, aiming to elucidate the following: (1) the histopathological alterations in the hepatopancreas under stress conditions; (2) the dynamics of the oxidative stress response in the hepatopancreas; (3) changes in the expression levels of genes related to immunity, detoxification, and endoplasmic reticulum stress in the hepatopancreas; and (4) the underlying mechanisms of metabolic reprogramming in the hepatopancreas. The findings will provide preliminary insights into the mechanisms by which nitrite and microplastic stress affect the physiological functions of the *P. vannamei* hepatopancreas, offering a theoretical foundation for promoting a healthier and more efficient shrimp aquaculture.

2. Materials and Methods

2.1. Chemicals

This study used green fluorescent polystyrene microspheres (5 μm in diameter, product code: CH2506-051) purchased from Qingdao Abate Co., Ltd., Qingdao, China. A

concentrated stock suspension was prepared by dispersing the microspheres in deionized water. Prior to each exposure experiment, the working suspension was sonicated for 10 min to minimize aggregation and ensure even dispersion before being added to the tanks at the target concentration.

2.2. Shrimp

Juvenile *P. vannamei* with an average body weight of 6.3 ± 0.2 g were sourced from the Shenzhen Base of the South China Sea Fisheries Research Institute. Prior to the stress experiment, the shrimp were acclimated for 7 days in a 200 L fiberglass tank. The water conditions, including a temperature of 30 ± 0.5 °C, a salinity of 30‰, a pH of 7.8–8.0, and continuous aeration for 24 h, were maintained to ensure suitability for the shrimp. Daily, 50% of the water was changed, and the shrimp were fed compound feed at 5% of their body weight. Additionally, the concentrations of ammonia, nitrogen, and nitrite were measured using a spectrophotometer. Measurements were taken 1 h after water renewal to ensure complete dissolution of the reagents in the experimental water.

2.3. Exposure Design and Sample Collection

Following 7 days of acclimation, the healthy shrimp were randomly assigned to 4 groups: the control group (CK), 20 mg·L^{-1} NO_2^--N (nitrite-nitrogen) nitrite group (NIT), 10 μg·L^{-1} microplastic group (MP), and 20 mg·L^{-1} nitrite and 10 μg·L^{-1} microplastic group (NM). Each group contained 3 replicate tanks, with 30 shrimp per tank. Nitrite levels were monitored every 24 h and adjusted as necessary. To maintain consistent stress conditions, the water was completely replaced every two days, with appropriate concentrations of nitrite or microspheres replenished. Aside from the stressors, all other culture conditions mirrored those of the adaptation phase, and the stress exposure experiment lasted for 14 days.

The hepatopancreases of six shrimp per tank were sampled and pooled for oxidative enzyme activity analysis, and six shrimp were similarly sampled for gene expression analysis. Gene expression samples were stored in RNA protection solution (RNAFollow, NCM Biotech, Suzhou, China) at 4 °C for 24 h, and then stored at −80 °C. Samples used for metabolomics analysis were taken from the hepatopancreas of six shrimp in each tank, mixed, and stored at −80 °C.

2.4. Histopathological Analysis

The tissue section preparation method was performed as described in our previous study [17]. After fixing the hepatopancreatic tissue in formalin solution for 24 h, it was rinsed with deionized water for 30 min and then dehydrated with a gradient of ethanol (70%, 80%, 90%, and 100%). Serial paraffin sections of the hepatopancreatic tissue were prepared, with each sample sectioned 10 times at 100 μm intervals, followed by hematoxylin-eosin (HE) staining to assess the effects of microplastics and nitrites on tissue morphology. Histopathological alterations were examined using a microscope (Olympus, Tokyo, Japan) at 400× magnification. The histological assessment was conducted qualitatively through systematic observation. Two researchers independently evaluated the sections, focusing on key morphological features including lumen dilation and integrity, vacuolization, hepatic tubule atrophy, changes in B-cell and R-cell populations, and basement membrane integrity. The observations were then compared, and a consensus description was reached for each sample. This approach aimed to characterize the pattern and extent of tissue damage across different treatment groups.

2.5. Biochemical Assays

Sterile phosphate-buffered saline (PBS) at 4 °C was added to shrimp hepatopancreas samples and homogenized to obtain a 10% crude tissue solution. After aliquoting the tissue homogenates by group, each individual sample in each group was divided into two technical replicates for analysis, with each technical replicate subjected to 3–4 measurements. Biochemical parameters, including catalase (CAT), superoxide dismutase (SOD), lipid peroxidation (LPO), hydrogen peroxide (H_2O_2), malondialdehyde (MDA), and superoxide anion (O_2^-), were determined using the supernatant after homogenization and centrifugation. All reagents were purchased from Nanjing Jiancheng Bioengineering Institute (Nanjing, Jiangsu, China), with the corresponding kit catalog numbers listed as follows: CAT (A007-1-1), SOD (A001-1-1), LPO (A106-1-2), O_2^- (Y002-1-1), H2O2 (A064-5-1), and MDA (A003-1-1).

2.6. mRNA Expression Levels of Hepatopancreas

Total RNA was extracted from the hepatopancreas of shrimp thawed at 4 °C using the Trizol method. To improve RNA purity, genomic DNA was removed using DNase, and the purified RNA was reverse transcribed into cDNA in an RNase-free system. The expression levels of immune and detoxification metabolic genes were detected by RT-qPCR (Table S1) and calculated using the $2^{-\Delta\Delta}$CT method. *β-actin* from *P. vannamei* was selected as the internal control gene. The relative expression levels of immune and detoxification metabolic genes in each experimental group were calculated using the control group (CK group) as the baseline. The amplification efficiency for all primers (including both reference and target genes) ranged between 95% and 105%, with standard curve correlation coefficients (R^2) all greater than 0.99, meeting the requirements for reliable quantification. The reaction system and reaction procedure followed those outlined in Ref. [3]. All reactions were performed in triplicate. Ct values were calculated using QuantStudio™ design and analysis software (v1.5.2).

2.7. Metabolomics Analysis

After thawing at 4 °C, hepatopancreatic samples were used to extract metabolites using a methanol/chloroform/water mixture containing 2-chloro-1-phenylalanine (4 ppm) as an internal standard. Except for a 20 µL extract used for quality control (QC), all other extracts were analyzed by liquid chromatography–mass spectrometry (LC-MS; Thermo Fisher Scientific, Waltham, MA, USA). The analysis was performed on a Thermo Vanquish UHPLC (Thermo Fisher Scientific, Waltham, MA, USA) system coupled to a Thermo Orbitrap Exploris 120 mass spectrometer (Thermo Fisher Scientific, Waltham, MA, USA). Chromatographic separation was achieved on an ACQUITY UPLC® HSS T3 column (2.1 mm × 100 mm, 1.8 µm; Waters, Milford, MA, USA). Mass spectrometry was performed in full-scan MS/dd-MS^2 mode in both positive and negative ion modes. Metabolites were accurately identified by comparing MS/MS spectra with a standard database under conditions of <5 ppm mass error. Metabolites with a variable projection importance (VIP) score > 1.0 and a p-value < 0.05 (Student's t-test) and $|\log_2(\text{fold change})| > 0$ under different experimental conditions were considered differentially expressed metabolites. Specific sample preparation methods and detailed analytical procedures are provided in the Supplementary Materials.

2.8. Statistical Analysis

The relative expression levels of immune and detoxification genes are expressed as mean ± standard deviation (SD). Statistical analysis of the data between groups was performed using SPSS 26.0 software with one-way ANOVA. The data were confirmed to be normally distributed using t-tests; a p-value > 0.05 was considered normal. Homogeneity of variance was confirmed using Levene's test; a p-value > 0.05 was considered homogeneous.

The least significant difference (LSD) test was used to test the significance of differences within and between groups. The statistical significance level was set at p-value < 0.05.

3. Results

3.1. Morphological Changes

The hepatic tubules, lumens, and cell structures of the hepatopancreas in the CK group appeared normal. The hepatopancreatic tubules are composed of several key cell types: B cells (secretory cells) are responsible for synthesizing and secreting digestive enzymes; R cells (storage cells) primarily store nutrients, such as lipids and glycogen, and may also participate in detoxification; F cells (fiber cells) are thought to provide structural support. These cells rest on a basement membrane (BM), which offers structural and functional support to the epithelium. The central lumen (L) serves as a channel for the transport of digestive products. Additionally, transferred vacuoles (TV) are involved in intracellular transport and secretion processes.

Compared to the CK group, significant histopathological alterations were observed in all stress groups. The stellate lumen expanded in both the NIT and MP groups, accompanied by the appearance and rupture of vacuoles, leading to a thinner epithelial cell layer. Additionally, the hepatic tubular tissues in each stress group exhibited atrophy and deformation. Specifically, in the NIT group, the number of R cells increased while the number of B cells decreased (Table S3). Cytoplasmic basophilia was increased, alongside nuclear and nucleolar hypertrophy, while a decrease in glandular cell vacuolization was noted. In the MP group, both R cells and B cells decreased. The lumens were enlarged and lysed. The tubules exhibited signs of necrosis, characterized by wider inter-tubular spaces, the disappearance of cytoplasmic vacuolization, and the presence of pyknotic nuclei. In the NM group (combined stress), a decrease in both R and B cells was also observed. Furthermore, the basement membrane suffered evident damage, displaying detachment from the glandular epithelium. Similarly to the NIT group, increased cytoplasmic basophilia and decreased cytoplasmic vacuolization were prominent features in this group (Figure 1A–D).

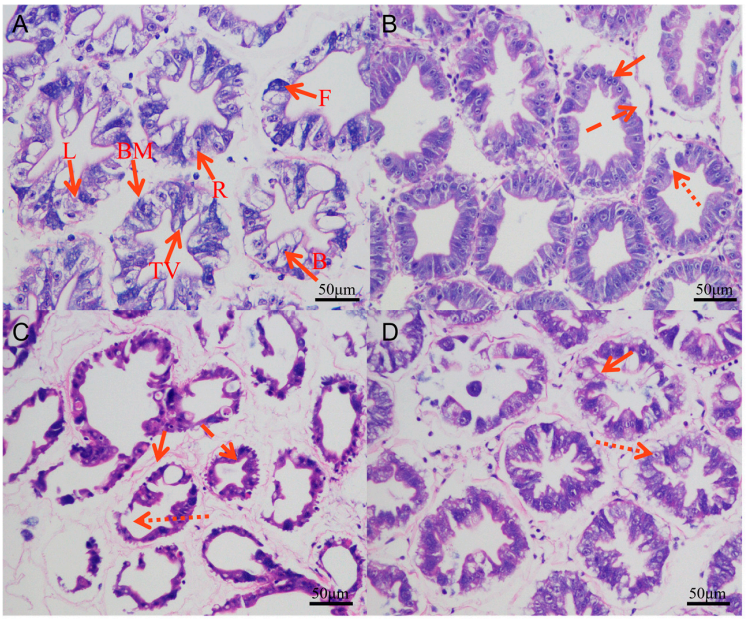


Figure 1. Histological alterations in the hepatopancreas of *P. vannamei* after nitrite and microplastics exposure. (**A**) CK group; (**B**) NIT group; (**C**) MP group; (**D**) NM group. B—secretory cells (B cells); R—storage cells (R cells); F—fiber cells; BM—basement membrane; L—lumen; TV—transferred vacuoles. Solid arrows (decreased number of R cells and B cells); dashed arrows (hepatic tubular atrophy deformation); dotted arrows (basement membrane damage).

3.2. Changes in Oxidative Enzyme Activity in the Shrimp Hepatopancreas

Compared to the CK group, CAT activity significantly increased in the NIT and NM groups ($p < 0.05$). SOD activity showed a significant increase in the MP group, but significantly decreased in the NM group ($p < 0.05$). Although SOD activity increased in the NIT and MP groups, the difference was not significant ($p > 0.05$). The LPO activity increased in all experimental groups, but there was a significant difference only in the NM group. The contents of O_2^- and MDA significantly increased in all three stress groups ($p < 0.05$), with the NM group exhibiting the highest levels. H_2O_2 content significantly increased in the NIT and NM groups ($p < 0.05$, Figure 2A–F).

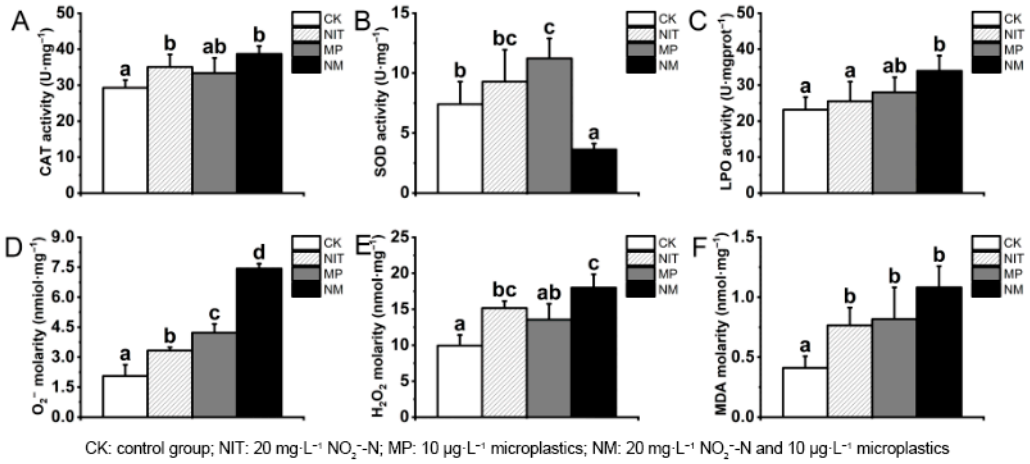


Figure 2. Oxidative stress indexes in the hepatopancreas of *P. vannamei* after nitrite and microplastics exposure. (**A**) CAT activity; (**B**) SOD; (**C**) LPO; (**D**) O_2^-; (**E**) H_2O_2; (**F**) MDA. Each treatment group consisted of three replicates of six hepatopancreas ($n = 3$ tanks/6 hepatopancreas). Different letters above the error bars indicate statistically significant differences among groups ($p < 0.05$), whereas identical letters denote no significant differences ($p > 0.05$).

3.3. Changes in Antioxidant Gene Expression Level

Compared to the CK group, the relative expression levels of the ROS regulator-1 (*ROMO1*) gene significantly increased in the NIT group ($p < 0.05$). The relative expression level of the *SOD* gene significantly increased in the MP and NM groups ($p < 0.05$). Additionally, the relative expression level of glutathione peroxidase (*GPx*) gene significantly increased in both the NIT and MP groups ($p < 0.05$). Moreover, the relative expression level of the thioredoxin (*Trx*) gene significantly increased in the three stress groups ($p < 0.05$, Figure 3A).

3.4. Changes in Immune Gene Expression Level

Compared to the CK group, the relative expression levels of the cytochrome oxidase (*cytC*), apoptosis factor caspase-3 (*CASP-3*), and antimicrobial peptide crustin (*Crus*) genes were significantly elevated in the three stress groups ($p < 0.05$). Conversely, the relative expression level of the anti-lipopolysaccharide factor (*ALF*) gene significantly decreased in the NM group ($p < 0.05$), with a decreasing trend observed in the NIT and MP groups, although not statistically significant ($p > 0.05$). Moreover, the relative expression level of the prophenoloxidase (*proPO*) gene significantly increased in the NM group ($p < 0.05$) (Figure 3B).

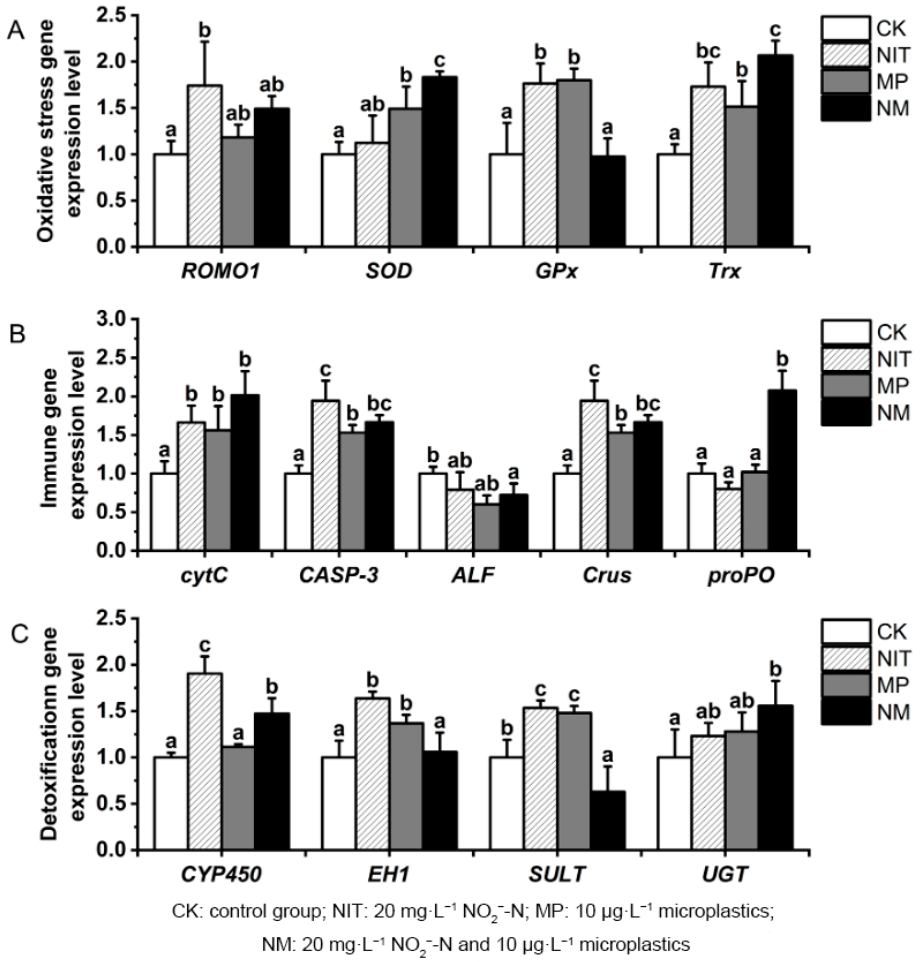


Figure 3. Effects of nitrite and microplastics stress on the mRNA expression levels of physiological indexes in the hepatopancreas of *P. vannamei.* Six shrimp in each group were randomly selected for measurement (n = 3 tanks/6 hepatopancreas). (**A**) Antioxidant gene expression levels; (**B**) immune gene expression levels; (**C**) detoxification metabolic gene expression levels. Different letters above the error bars indicate statistically significant differences among groups ($p < 0.05$), whereas identical letters denote no significant differences ($p > 0.05$).

3.5. Changes in Detoxification Metabolic Gene Expression Level

Compared to the CK group, the relative expression level of the cytochrome P450 enzyme (*CYP450*) gene was significantly elevated in the NIT and NM groups ($p < 0.05$, Figure 3C and Table S2). The relative expression level of the epoxide hydrolas (*EH1*) gene significantly increased in NIT and MP groups ($p < 0.05$). Additionally, the relative expression level of the sulfo-transferase (*SULT*) gene significantly increased in the NIT and MP groups but significantly decreased in the NM group ($p < 0.05$). Furthermore, the relative expression level of the uridine diphosphate glucuronosyltransferase (*UGT*) gene significantly increased in the NM group ($p < 0.05$), and showed a tendency to increase in the NIT and MP groups, although the difference was not significant ($p > 0.05$).

3.6. Metabolic Function Variations

3.6.1. Identification of Differential Metabolites

We investigated changes in the metabolic patterns of the hepatopancreas under stress. Positive and negative ion base peak chromatograms showed significant differences in metabolic patterns among the three stress groups compared to the CK group (Figure S1A,B). Additionally, the Orthogonal Partial Least Squares–Discriminant Analysis (OPLS-DA) score plot demonstrated significant separation between the three stress groups and the CK group,

indicating that both nitrite and microplastic stress can induce changes in the metabolic phenotype of the hepatopancreas (Figure 4A,B).

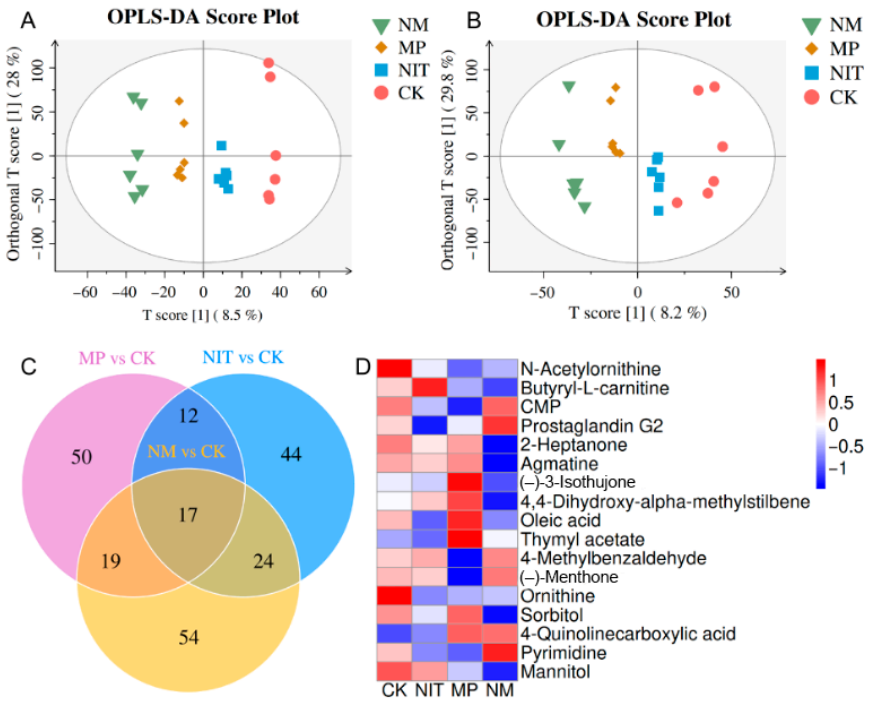


Figure 4. The analysis of metabolic pattern variation and differential metabolites in the hepatopancreas of *P. vannamei* after nitrite and microplastic stress (n = 2 × (3 tanks/6 hepatopancreas), which is similar in Figures 5 and 6). (**A**) Negative ion mode of multivariate statistical analysis of OPLS-DA; (**B**) positive ion mode of multivariate statistical analysis of OPLS-DA; (**C**) Venn analysis of differential metabolites between the different groups; (**D**) the significantly altered differential metabolite markers.

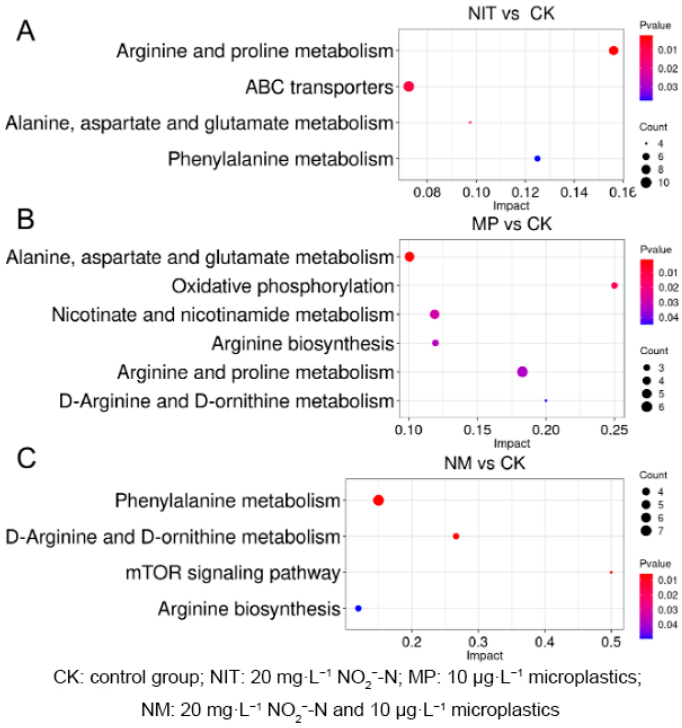


Figure 5. The pathways of differential metabolites in the hepatopancreas of *P. vannamei.* (**A**) NIT vs. CK; (**B**) MP vs. CK; (**C**) NM vs. CK.

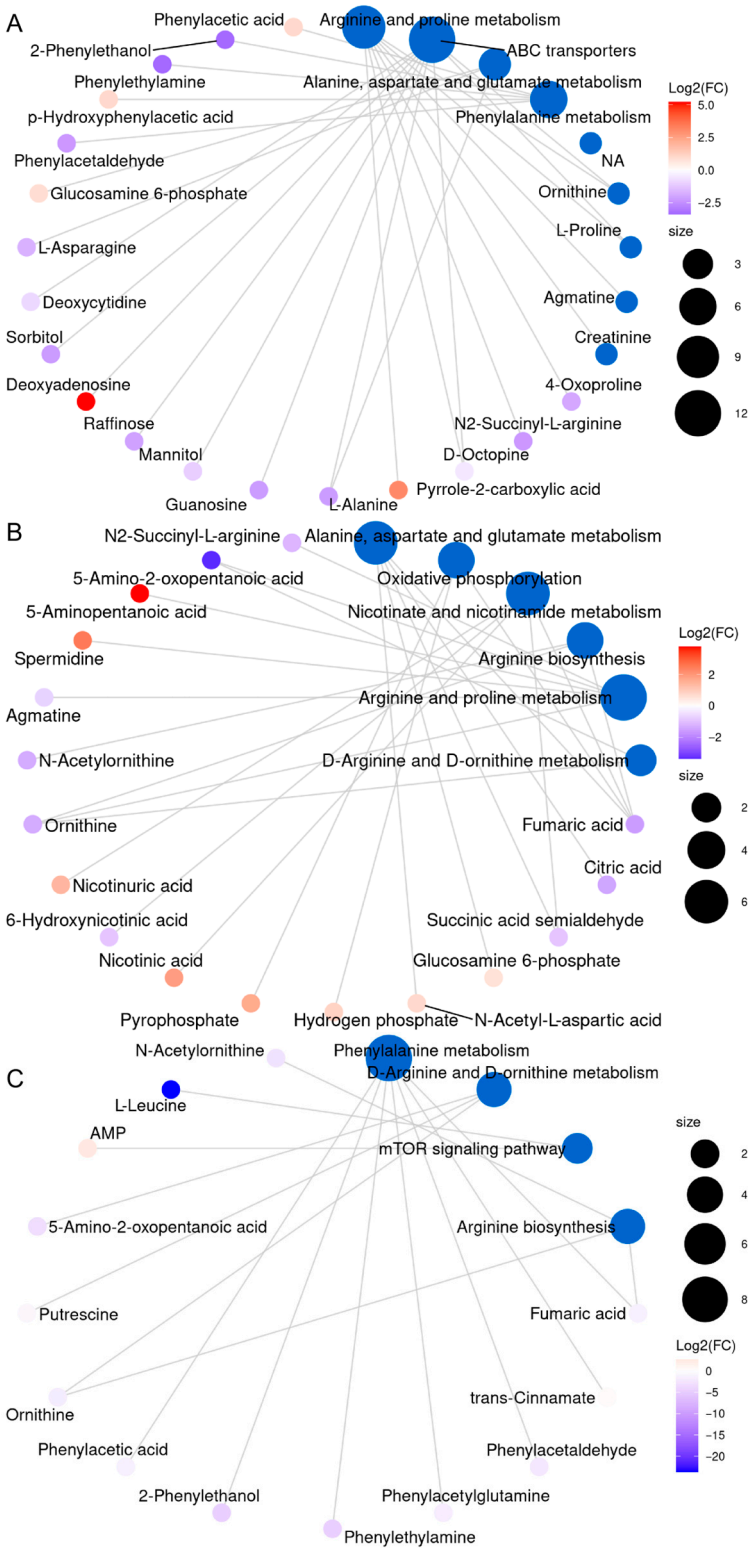


Figure 6. Correlation network of the metabolic pathways in the hepatopancreas of *P. vannamei*. (**A**) NIT vs. CK; (**B**) MP vs. CK; (**C**) NM vs. CK. Nodes: pathway; node size: impact value correlations.

The 221 differential metabolites were screened from the three stress groups compared to the CK group, primarily comprising amino acids and their derivatives, fatty acids, and other compounds (Figure 4C). Specifically, the NIT group had 56 differentially expressed metabolites, with 19 upregulated and 37 downregulated; the MP group had 68 differentially expressed metabolites, with 24 upregulated and 44 downregulated; and the NM group had 75 differentially expressed metabolites, with 24 upregulated and 51 downregulated

(Figure 4D). Additionally, the Venn diagram shows 17 metabolites common to all three stress groups, including 2-heptanone, 4,4-dihydroxy-α-methylstilbene, 4-methylbenzaldehyde, 4-quinolinecarboxylic acid, spermine, butyryl-L-carnitine, mannitol, N-acetylornithine deacylase, oleic acid, ornithine, pyrimidine, sorbitol, and thymol acetate.

3.6.2. Functional Analysis of Differential Metabolites

Differentially enriched metabolic pathways were analyzed across the three stress groups ($p < 0.05$, Figure 5). Among them, arginine and proline metabolism, as well as alanine, aspartate, and glutamate metabolism, were highly enriched in the NIT and MP groups, and phenylalanine metabolism was highly enriched in the NIT and NM groups. Arginine biosynthesis and D-arginine and D-ornithine metabolism were highly enriched in the MP and NM groups. Additionally, the ABC transporter pathway was highly enriched only in the NIT group; the oxidative phosphorylation pathway was highly enriched only in the MP group; the mTOR signaling pathway was highly enriched only in the NM group.

Metabolic pathway correlation network analysis showed that in the NIT group, arginine and proline metabolism, ABC transporters, and alanine, aspartate, and glutamate metabolism were associated with D-octopine, Ornithine, and L-Alanine, and their content decreased (Figure 6). In the MP group, arginine and proline metabolism; D-arginine and D-ornithine metabolism; arginine biosynthesis; alanine, aspartate, and glutamate metabolism; oxidative phosphorylation; and nicotinate and nicotinamide metabolism were associated with 5-amino-2-oxopentanoic acid, ornithine, fumaric acid, and succinic acid semialdehyde, and the content of the above substances decreased. In the NM group, D-arginine and D-ornithine metabolism, arginine biosynthesis, and phenylalanine metabolism were associated with ornithine and fumaric acid, and their contents decreased.

3.6.3. Characteristics of Metabolite Markers

The stress-related metabolite biomarkers were further identified (Table 1). Among the six lipid metabolites, oleic acid and prostaglandin G2 decreased in all three stress groups; linoleic acid and docosapentaenoic acid decreased in the MP group; palmitic acid content increased in the NIT group; and docosahexaenoic acid content increased in the MP group. Among the six amino acid substances, agmatine, ornithine, and N-acetylornithine decreased in all three stress groups, decreased in the NIT and NM groups, but increased in the MP group; L-leucine decreased in the MP and NM groups; L-Arginine and L-Tyrosine increased in the MP and NM groups. Among the five carbohydrates, sorbitol decreased in all three stress groups; D-mannose and glyceric acid increased in the MP group. In addition, the key node metabolites of the citric acid cycle, such as citric acid and fumaric acid, decreased in the MP and NM groups.

Table 1. Changes in the content of biomarkers of hepatopancreatic metabolites in *P. vannamei*.

Metabolites	Log2 Fold Change			Categories
	NIT vs. CK	MP vs. CK	NM vs. CK	
Oleic acid	−2.54	−3.15	−2.85	Lipid
Prostaglandin G2	−2.78	−2.46	−5.20	Lipid
Linoleic acid	0	−1.44	0	Lipid
Palmitic acid	1.28	0	0	Lipid
Docosahexaenoic acid	0	1.09	0	Lipid
Docosapentaenoic acid	0	−2.36	0	Lipid
L-Leucine	0	−2.72	−1.13	Amino acid
Agmatine	−0.89	−0.71	−0.6	Amino acid

Table 1. *Cont.*

Metabolites	Log2 Fold Change			Categories
	NIT vs. CK	MP vs. CK	NM vs. CK	
L-Arginine	0	3.37	0.84	Amino acid
L-Tyrosine	0	1.39	2.80	Amino acid
Ornithine	−1.55	−1.45	−2.87	Amino acid
N-Acetylornithine	−1.95	−1.38	−2.74	Amino acid
Glyceric acid	0	1.26	0	Carbohydrate
Citric acid	0	−1.46	−1.63	Carbohydrate
D-Mannose	0	0.72	0	Carbohydrate
Sorbitol	−2.24	−2.04	−2.41	Carbohydrate
Fumaric acid	0	−1.56	−1.41	Carbohydrate

4. Discussion

4.1. Changes in Hepatopancreas Morphology in Response to Nitrite and Microplastics Exposure

The hepatopancreas serves as a crucial organ for detoxification, excretion, and metabolism in shrimp. Structural changes in this organ reflect the level of physiological function [21]. Environmental pollutants such as microplastics and algal toxins tend to accumulate most in the hepatopancreas [22]. Research indicated that following 72 h of exposure to 20 mg·L^{-1} nitrite stress, the number and volume of hepatopancreatic B cells and transport vesicles in *P. vannamei* increased [23]. Additionally, exposure to microplastics at varying concentrations led to hepatopancreatic tubular atrophy and blood cell rupture in *P. vannamei* [24]. Exposure to nitrite and microplastic stress individually resulted in atrophied and deformed hepatic tubular tissues, accompanied by the appearance and rupture of vacuoles. Moreover, combined stress led to a reduction in R- and B-cell populations and rupture of the basement membrane. These findings suggested that nitrite and microplastic stress impaired the structural integrity and disrupted the physiological function of the hepatopancreas. Furthermore, the damage to the hepatopancreatic tissue was more pronounced under dual stress, indicating that concurrent exposure exacerbated the toxic effects of nitrite and microplastics.

4.2. Hepatopancreas Physiological Responses to Nitrite and Microplastics Exposure

Oxidative stress can be induced by environmental pollutants and factors that trigger the production of excessive ROS. Organisms depend on antioxidant enzymes like SOD, CAT, and GPx to uphold redox homeostasis [24]. In this study, CAT activity and LPO content increased, while *ROMO1*, *SOD*, and *Trx* gene expression levels were elevated, along with an increase in *GPx* gene expression in the NIT and MP groups. These findings suggested that the presence of nitrites and microplastics, alone or simultaneously, can induce oxidative stress and impair the antioxidant function of the shrimp hepatopancreas.

Oxidative stress serves as a crucial trigger for apoptosis [25,26], and orderly apoptosis aids in maintaining intracellular environmental stability [27]. *Cytc* first binds to *Casp-9*, then activates *Casp-3*, leading to apoptosis [28]. Environmental factors disrupting internal homeostasis facilitate pathogen invasion and colonization. Microbial cell wall components activate *proPO*, contributing to defense responses [29]. Antimicrobial peptides, such as *ALF* and *Crus*, exhibit antibacterial activity and play pivotal roles in non-specific immune responses [30,31]. This study observed elevated expression levels of the *Cytc*, *Casp-3*, and *Crus* genes in both the MP and NM groups, along with an elevated *proPO* gene expression level. This suggests that the individual and combined stress of nitrite and microplastics induced the immune response in shrimp and affected the immune function of shrimp hepatopancreas.

CYP450 and *EH* belong to phase I metabolic enzymes [32], while *SULT* and *UGT* enzymes are classified as phase II metabolic enzymes [33], involved in the metabolism of exogenous substances within the body. Previous studies have demonstrated the involvement of *EH* in liver metabolism of arsenite [34]. This study observed elevated expression levels of the *CYP450*, *EH1*, and *UGT* genes, along with increased *SULT* gene expression in the NIT and MP groups and decreased expression in the NM group, suggesting that nitrite and microplastics induce detoxification metabolism in the hepatopancreas.

The endoplasmic reticulum plays a vital role in maintaining intracellular homeostasis. Various intracellular and extracellular factors inducing endoplasmic reticulum stress can disrupt its balance [35]. Bip binds to *PERK*, *ATF6*, and *IRE1* in non-stress cells, and dissociates from them during endoplasmic reticulum stress, activating the unfolded protein response [36]. Downstream molecules of this reaction, *eIF2α* and Beclin1, are implicated in apoptosis regulation [37]. In this study, *IRE1*, *ATF6*, *Beclin1*, and *eIF2α* genes exhibited increased expression levels in all stress groups, while *Bip* expression increased in the NIT and MP groups but decreased in the NM group, indicating that nitrite and microplastic stress induced endoplasmic reticulum stress in the hepatopancreas, which is detrimental to normal cellular function.

4.3. Hepatopancreas Metabolic Response to Nitrite and Microplastics Exposure

Non-targeted metabolomics revealed the changes in *P. vannamei* hepatopancreas metabolic patterns induced by the nitrite and microplastics stress. Under different stress conditions, the abundance of numerous metabolites changed, indicating that the metabolic function of the shrimp was significantly affected. More differential metabolites appeared under combined stress conditions, indicating that combined stress may have a greater impact. Of the metabolic pathways affected, most were related to amino acids. The arginine and proline metabolism and the alanine, aspartate, and glutamate metabolism pathways related to lipid anabolism and the tricarboxylic acid cycle are highly enriched in the nitrite and microplastic stress groups [38,39]. It shows that both nitrite and microplastic stress affect energy metabolism processes, such as those for lipids or sugars. However, the toxic mechanisms of nitrite and microplastics to shrimp are different. The phenylalanine metabolism involved in the regulation of glucose and lipid metabolism was significantly enriched in both the nitrite group and the combined stress group, and the D-arginine and D-ornithine metabolism related to non-specific immunity and energy supply were highly enriched in the MP group and the NM group [40,41]. This suggests that nitrite and microplastics affect the body's energy metabolism by different mechanisms. In addition, the ABC transporter pathway involved in the transport and detoxification of toxic molecules was only highly enriched in the NIT group, and the oxidative phosphorylation pathway related to mitochondrial production of ATP and ROS was only highly enriched in the MP group. This indicates that nitrite activated the shrimp's detoxification metabolism, while microplastics enhanced mitochondrial energy production efficiency, providing a theoretical basis for assessing environmental stress impacts on shrimp.

We further screened 18 metabolites with biomarker potential that are closely related to the health of shrimp hepatopancreas. Fatty acids represent the primary components of lipids and play a pivotal role in numerous life processes. n-3 polyunsaturated fatty acids (PUFAs) and n-6 PUFAs, including linoleic acid, docosapentaenoic acid, and docosahexaenoic acid, are not only essential for maintaining the fluidity of cell membranes but also regulate the immune response and provide energy through β-oxidation. Derivatives of these compounds, such as prostaglandins and oleic acid, also function in the regulation of inflammation [42,43]. In addition, palmitic acid plays an important role in autophagy and pathogen–host interaction. The observed decrease in the content of oleic acid and

prostaglandins in all experimental groups indicated that nitrite and microplastics inhibited the immune response process mediated by oleic acid and prostaglandins. In the MP group, the content of docosapentaenoic acid and linoleic acid decreased, while the content of docosahexaenoic acid increased, indicating that microplastics reduced the fluidity of the cell membrane and inhibited the immune regulation process. The increase in palmitic acid content in the NIT group indicates that nitrite activated the interaction between shrimp and pathogens, which may be related to the fact that NIT stress provides invasion conditions for opportunistic pathogens.

Among the seven amino acid substances, N-acetylornithine plays a role in the production of ornithine, which serves to prevent the formation of unsaturated fatty acid oxygen [44]. Agmatine inhibits inducible nitric oxide synthase (iNOS) [45]. In this study, the content of ornithine, N-acetylornithine, and agmatine decreased, indicating that nitrite and microplastics inhibited the antioxidant response and may cause oxidative damage to the hepatopancreas. L-leucine and L-tyrosine are involved in the production of acetyl-CoA [46], which in turn is involved in the tricarboxylic acid cycle and lipid synthesis [47,48]. L-arginine is involved in the synthesis of nitric oxide (NO) [49]. In this study, microplastics and combined stress induced a decrease in L-leucine content and an increase in L-tyrosine and L-arginine content, indicating that microplastics mainly caused the disorder of acetyl-CoA synthesis, which affected the synthesis and metabolism of energy substances and promoted NO synthesis.

The tricarboxylic acid cycle is the ultimate common pathway for the oxidation of carbohydrates, proteins, and lipids. Among the five carbohydrates, citric acid and fumaric acid are intermediates of the tricarboxylic acid cycle and participate in intracellular energy supply [50,51]. D-mannose and sorbitol at supraphysiological levels induce oxidative stress [52,53]. Glyceric acid is a metabolite of glycolysis [54]. In this study, the sorbitol content of each experimental group decreased, indicating that nitrite and microplastic stress inhibited oxidative stress response. The contents of citric acid and fumaric acid were mainly inhibited by microplastic stress, indicating that microplastics inhibited the tricarboxylic acid cycle and affected the energy supply of shrimp. Microplastics induced an increase in the content of D-mannose and glyceric acid, indicating that nitrite and microplastic stress may have impaired a specific antioxidant or osmoprotective pathway associated with sorbitol metabolism, potentially compromising the hepatopancreas's ability to counteract the ongoing oxidative challenge. While this study provides an initial investigation into the hepatopancreatic toxicity of co-existing nitrite and microplastics in *Penaeus vannamei*, it is not without limitations. Future studies should aim to delineate the toxic mechanisms more precisely by incorporating the following: (1) dose–response and time-course experiments to establish effect thresholds and temporal progression of damage; (2) ultrastructural analysis (e.g., transmission electron microscopy) to directly assess mitochondrial integrity and autophagic activity; and (3) functional assays, such as pharmacological inhibition or genetic manipulation of key proteins (e.g., in the mTOR pathway), to establish causal relationships between pathway disruption and hepatopancreatic dysfunction. All these adverse effects will ultimately have a negative impact not only on animal welfare, but also on the economic efficiency of this important species in global aquaculture.

5. Conclusions

The stress caused changes in oxidative stress and metabolic patterns in the hepatopancreas, inducing alterations in detoxification metabolism and immune-related genes, ultimately leading to damage to the integrity of the hepatopancreas (Figure 7). Detoxification metabolism and immune-related indicators were also affected by stress. Furthermore, disruption was observed in the homeostasis of the immune and energy metabolism systems,

accompanied by changes in metabolites, including lipids, amino acids, and carbohydrates. Nitrite stress induced physiological disorders in the hepatopancreas, which were exacerbated by microplastics. Hence, understanding the effects of environmental factors on farmed animals can be achieved by monitoring changes in physiological indices during the breeding process, facilitating timely adjustments to breeding strategies.

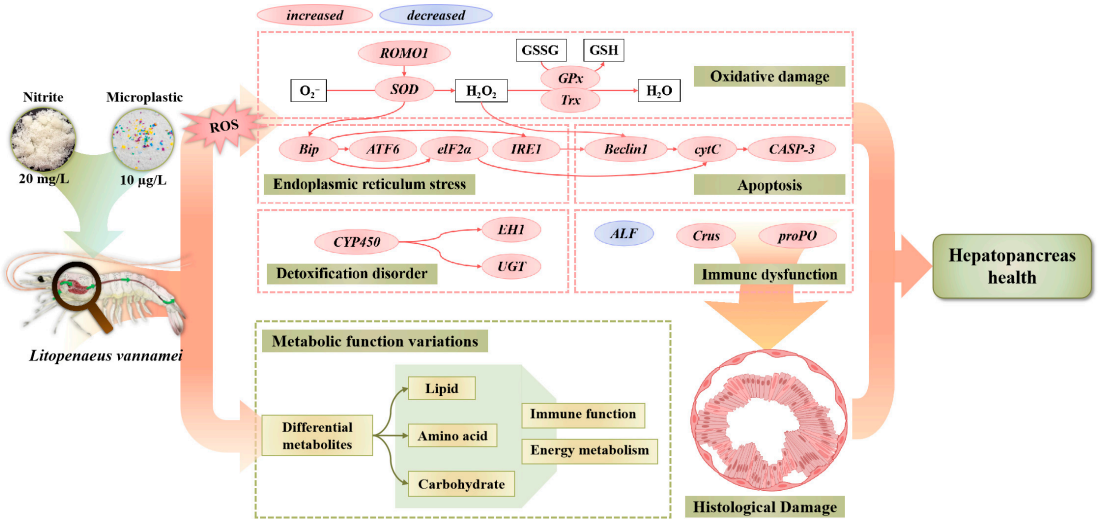


Figure 7. A schematic diagram illustrating the mechanism of toxicity of nitrites and microplastics to the hepatopancreas of *P. vannamei*.

Supplementary Materials: The following supporting information can be downloaded at: https://www.mdpi.com/article/10.3390/jox16010022/s1, Figure S1: Base peak chromatogram of the *P. vannamei* hepatopancreas samples using LC-MS analysis; Figure S2: The original images for Figure 1 that were arranged in the order of the experimental groups; Table S1: The RT qPCR primer sequences used in this study; Table S2: One-way ANOVA of nitrite and microplastics stress on the mRNA expression levels of physiological indexes in the hepatopancreas of *P. vannamei*; Table S3: The number of B cells in hepatopancreatic tissue.

Author Contributions: Y.-F.X. and X.-Y.Z.: Writing—original draft, Writing—review and editing. H.-B.D. and J.-H.H.: Software, Validation. J.-S.Z. and Y.-F.D.: Experimental design. All authors have read and agreed to the published version of the manuscript.

Funding: This study was supported by the Central Public-Interest Scientific Institution Basal Research Fund, South China Sea Fisheries Research Institute, CAFS (2024XT01); Guangzhou Science and Technology Plan Project (2025D04J0016); the Key Research and Development Program projects in Ningbo (2023Z113); the Fujian Special Fund for the Development of Marine and Fishery (FJHYF-L-2025-08); the National Key Research and Development Program of China (2023YFD2400403, 2023YFD2400705); the Guangdong Basic and Applied Basic Research Foundation (2024A1515030047); the Agricultural Research Outstanding Talents Training Program (13210308); the Guangdong Province Science and Technology Commissioner Supporting Village Project (KTP20240452); the Yangjiang Science and Technology Planning Project (SBQW2024005); the Central Public-Interest Scientific Institution Basal Research Fund, CAFS (2023TD97); and the China-ASEAN Maritime Cooperation Fund China-ASEAN Modern Marine Fishery Technical Cooperation, Industrialization Development and Demonstration.

Institutional Review Board Statement: The animal study protocol was approved by the Institution Animal Care and Use Committee of the South China Sea Fisheries Research Institute (protocol code SCSFRI-CAFS, No. nhdf2022-15) on 12 June 2022.

Informed Consent Statement: Not applicable.

Data Availability Statement: The original contributions presented in this study are included in the article/Supplementary Materials. Further inquiries can be directed to the corresponding authors.

Conflicts of Interest: The authors declare no conflicts of interest.

References

1. Fajardo, C.; Martinez-Rodriguez, G.; Costas, B.; Mancera, J.M.; Fernandez-Boo, S.; Rodulfo, H.; De Donato, M. Shrimp immune response: A transcriptomic perspective. *Rev. Aquac.* **2022**, *14*, 1136–1149. [CrossRef]
2. Fisheries Department, Agriculture Organization of the United Nations. *The State of World Fisheries and Aquaculture*; Food and Agriculture Organization of the United Nations: Rome, Italy, 2018.
3. Duan, Y.; Zhang, Y.; Dong, H.; Wang, Y.; Zheng, X.; Zhang, J. Effect of dietary *Clostridium butyricum* on growth, intestine health status and resistance to ammonia stress in Pacific white shrimp *Litopenaeus vannamei*. *Fish Shellfish Immunol.* **2017**, *65*, 25–33. [CrossRef]
4. Yu, J.L.; Ji, X.S.; Wang, X.P.; Li, T.M.; Wang, H.; Zeng, Q.F. Identification and characterization of differentially expressed genes in hepatopancreas of oriental river prawn *Macrobrachium nipponense* under nitrite stress. *Fish Shellfish Immunol.* **2019**, *87*, 144–154. [CrossRef]
5. Ugwu, K.; Herrera, A.; Gómez, M. Microplastics in marine biota: A review. *Mar. Pollut. Bull.* **2021**, *169*, 112540. [CrossRef]
6. Le, V.G.; Nguyen, M.K.; Ngo, H.H.; Barceló, D.; Nguyen, H.L.; Um, M.J.; Nguyen, D.D. Microplastics in aquaculture environments: Current occurrence, adverse effects, ecological risk, and nature-based mitigation solutions. *Mar. Pollut. Bull.* **2024**, *209*, 117168. [CrossRef]
7. Yu, Y.; Hu, L.; Tian, D.; Yu, Y.; Lu, L.; Zhang, J.; Huang, X.; Yan, M.; Chen, L.; Wu, Z.; et al. Toxicities of polystyrene microplastics (MPs) and hexabromocyclododecane (HBCD), alone or in combination, to the hepatopancreas of the whiteleg shrimp, *Litopenaeus vannamei*. *Environ. Pollut.* **2023**, *329*, 121646. [CrossRef]
8. Zeng, Y.; Deng, B.; Kang, Z.; Araujo, P.; Mjøs, S.A.; Liu, R.; Lin, J.; Yang, T.; Qu, Y. Tissue accumulation of polystyrene microplastics causes oxidative stress, hepatopancreatic injury and metabolome alterations in *Litopenaeus vannamei*. *Ecotoxicol. Environ. Saf.* **2023**, *256*, 114871. [CrossRef]
9. Romano, N.; Zeng, C. Toxic effects of ammonia, nitrite, and nitrate to decapod crustaceans: A review on factors influencing their toxicity, physiological consequences, and coping mechanisms. *Rev. Fish. Sci.* **2013**, *21*, 1–21. [CrossRef]
10. Sookruksawong, S.; Pongsomboon, S.; Tassanakajon, A. Genomic organization of the cytosolic manganese superoxide dismutase gene from the Pacific white shrimp, *Litopenaeus vannamei*, and its response to thermal stress. *Fish Shellfish Immunol.* **2013**, *35*, 1395–1405. [CrossRef] [PubMed]
11. Porter, A.; Godbold, J.A.; Lewis, C.N.; Savage, G.; Solan, M.; Galloway, T.S. Microplastic burden in marine benthic invertebrates depends on species traits and feeding ecology within biogeographical provinces. *Nat. Commun.* **2023**, *14*, 8023. [CrossRef] [PubMed]
12. Gray, A.D.; Weinstein, J.E. Size- and shape-dependent effects of microplastic particles on adult daggerblade grass shrimp (*Palaemonetes pugio*). *Environ. Toxicol. Chem.* **2017**, *36*, 3074–3080. [CrossRef]
13. Yin, J.; Li, J.; Craig, N.J.; Su, L. Microplastic pollution in wild populations of decapod crustaceans: A review. *Chemosphere* **2022**, *291*, 132985. [CrossRef]
14. Xing, Y.; Zhu, X.; Duan, Y.; Huang, J.; Nan, Y.; Zhang, J. Toxic effects of nitrite and microplastics stress on histology, oxidative stress, and metabolic function in the gills of Pacific white shrimp, *Litopenaeus vannamei*. *Mar. Pollut. Bull.* **2023**, *187*, 114531. [CrossRef]
15. Moncrieffe, R.; Masry, M.; Cai, B.; Rossignol, S.; Kamari, A.; Poirier, L.; Bertrand, S.; Wong-Wah-Chung, P.; Zalouk-Vergnoux, A. Study of the ageing and the sorption of polyaromatic hydrocarbons as influencing factors on the effects of microplastics on blue mussel. *Aquat. Toxicol.* **2023**, *262*, 106669. [CrossRef] [PubMed]
16. Duan, Y.; Zhang, J.; Huang, J.; Jiang, S. Effects of dietary *Clostridium butyricum* on the growth, digestive enzyme activity, antioxidant capacity, and resistance to nitrite stress of *Penaeus monodon*. *Probiotics Antimicrob. Proteins* **2019**, *11*, 938–945. [CrossRef] [PubMed]
17. Duan, Y.F.; Wang, Y.; Huang, J.H.; Li, H.; Dong, H.B.; Zhang, J.S. Toxic effects of cadmium and lead exposure on intestinal histology, oxidative stress response, and microbial community of Pacific white shrimp *Litopenaeus vannamei*. *Mar. Pollut. Bull.* **2021**, *167*, 112222. [CrossRef]
18. Hsieh, S.L.; Wu, Y.C.; Xu, R.Q.; Chen, Y.T.; Chen, C.W.; Singhania, R.R.; Dong, C.D. Effect of polyethylene microplastics on oxidative stress and histopathology damages in *Litopenaeus vannamei*. *Environ. Pollut.* **2021**, *288*, 117800. [CrossRef]
19. Zheng, J.; Li, C.; Zheng, X. Toxic effects of polystyrene microplastics on the intestine of *Amphioctopus fangsiao* (Mollusca: Cephalopoda): From physiological responses to underlying molecular mechanisms. *Chemosphere* **2022**, *308*, 136362. [CrossRef]
20. Zhang, J.M.; Fu, B.; Li, Y.; Sun, J.; Xie, J.; Wang, G.; Tian, J.; Kaneko, G.; Yu, E. The effect of nitrite and nitrate treatment on growth performance, nutritional composition and flavor-associated metabolites of grass carp (*Ctenopharyngodon idella*). *Aquaculture* **2023**, *562*, 738784. [CrossRef]

21. Han, S.; Wang, M.; Wang, B.; Liu, M.; Jiang, K.; Wang, L. A comparative study on oxidative stress response in the hepatopancreas and midgut of the white shrimp *Litopenaeus vannamei* under gradual changes to low or high pH environment. *Fish Shellfish Immunol.* **2018**, *76*, 27–34. [CrossRef]
22. Duan, Y.; Xiong, D.; Wang, Y.; Zhang, Z.; Li, H.; Dong, H.; Zhang, J. Toxicological effects of microplastics in *Litopenaeus vannamei* as indicated by an integrated microbiome, proteomic and metabolomic approach. *Sci. Total Environ.* **2021**, *761*, 143311. [CrossRef]
23. Ciji, A.; Akhtar, M.S. Nitrite implications and its management strategies in aquaculture: A review. *Rev. Aquac.* **2020**, *12*, 878–908. [CrossRef]
24. Rochman, C.M.; Browne, M.A. Classify plastic waste as hazardous: Policies for managing plastic debris are outdated and threaten the health of people and wildlife. *Nature* **2013**, *494*, 169. [CrossRef]
25. Cui, J.W.; Zhou, Q.; Yu, M.J.; Liu, Y.H.; Teng, X.H.; Gu, X.H. 4-tert-butylphenol triggers common carp hepatocytes ferroptosis via oxidative stress, iron overload, SLC7A11/GSH/GPX4 axis, and ATF4/HSPA5/GPX4 axis. *Ecotoxicol. Environ. Saf.* **2022**, *242*, 113944. [CrossRef]
26. Cheng, C.; Su, Y.; Ma, H.; Deng, Y.; Feng, J.; Chen, X.; Jie, Y.; Guo, Z. Effect of nitrite exposure on oxidative stress, DNA damage and apoptosis in mud crab (*Scylla paramamosain*). *Chemosphere* **2020**, *239*, 124668. [CrossRef]
27. Danial, N.N.; Korsmeyer, S.J. Cell death: Critical control points. *Cell* **2004**, *116*, 205–219. [CrossRef] [PubMed]
28. Cheng, S.; Chen, J. Effects of nitrite exposure on the hemolymph electrolyte, respiratory protein and free amino acid levels and water content of *Penaeus japonicus*. *Aquat. Toxicol.* **1998**, *44*, 129–139. [CrossRef]
29. Ai, H.; Huang, Y.; Li, S.; Weng, S.; Yu, X.; He, J. Characterization of a prophenoloxidase from hemocytes of the shrimp *Litopenaeus vannamei* that is down-regulated by white spot syndrome virus. *Fish Shellfish Immunol.* **2008**, *25*, 28–39. [CrossRef]
30. Amparyup, P.; Kondo, H.; Hirono, I.; Aoki, T.; Tassanakajon, A. Molecular cloning, genomic organization and recombinant expression of a crustin-like antimicrobial peptide from black tiger shrimp *Penaeus monodon*. *Mol. Immunol.* **2008**, *45*, 1085–1093. [CrossRef]
31. Liu, C.; Chung, C.; Lin, C.; Sung, H. Function of an anti-lipopolysaccharide factor (ALF) isoform isolated from the hemocytes of the giant freshwater prawn *Macrobrachium rosenbergii* in protecting against bacterial infection. *J. Invertebr. Pathol.* **2014**, *116*, 1–7. [CrossRef] [PubMed]
32. Patel, J.M.; Wolf, C.R.; Philpot, R.M. Interaction of 4-methylbenzaldehyde with rabbit pulmonary cytochrome P-450 in the intact animal, microsomes, and purified systems. Destructive and protective reactions. *Biochem. Pharmacol.* **1979**, *28*, 2031. [CrossRef]
33. Tatarinov, D.A.; Osipova, V.I.; Bogdanov, A.V.; Krivolapov, D.B.; Voloshina, A.D.; Mironov, V.F. ChemInform abstract: Synthesis of new 2-[2-(Dialkyl(diaryl)-phosphoryl)-2-methylpropyl] quinoline-4-carboxylic acids. *Chem. Heterocycl. Compd.* **2016**, *47*, 717–722. [CrossRef]
34. Thompson, E.D.; Burwinkel, K.E.; Chava, A.K.; Notch, E.G.; Mayer, G.D. Activity of Phase I and Phase II enzymes of the benzo[a]pyrene transformation pathway in zebrafish (*Danio rerio*) following waterborne exposure to arsenite. *Comp. Biochem. Physiol. Part C Toxicol. Pharmacol.* **2010**, *152*, 371–378. [CrossRef] [PubMed]
35. Topal, A.; Özdemir, S.; Arslan, H.; Çomaklı, S. How does elevated water temperature affect fish brain? (A neurophysiological and experimental study: Assessment of brain derived neurotrophic factor, cFOS, apoptotic genes, heat shock genes, ER-stress genes and oxidative stress genes). *Fish Shellfish Immunol.* **2021**, *115*, 198–204. [CrossRef]
36. Ning, B.; Zhang, Q.; Wang, N.; Deng, M.; Fang, Y. β-Asarone regulates ER stress and autophagy via inhibition of the PERK/CHOP/Bcl-2/Beclin-1 pathway in 6-OHDA-induced parkinsonian rats. *Neurochem. Res.* **2019**, *44*, 1159–1166. [CrossRef]
37. Xu, J.; Ruan, L.; Shi, H. eIF2α of *Litopenaeus vannamei* involved in shrimp immune response to WSSV infection. *Fish Shellfish Immunol.* **2014**, *40*, 609–615. [CrossRef] [PubMed]
38. Figueiredo-Silva, A.C.; Corraze, G.; Kaushik, S.; Peleteiro, J.B.; Valente, L.M. Modulation of blackspot seabream (*Pagellus bogaraveo*) intermediary metabolic pathways by dispensable amino acids. *Amino Acids* **2010**, *39*, 1401–1416. [CrossRef] [PubMed]
39. Szlas, A.; Kurek, J.M.; Krejpcio, Z. The Potential of L-arginine in prevention and treatment of disturbed carbohydrate and lipid metabolism-a review. *Nutrients* **2022**, *14*, 961. [CrossRef]
40. Guo, C.; Zhang, X.; Xie, S.; Luo, J.; Zhu, T.; Yang, Y.; Li, X.; Huang, C.; Dang, Y.; Zhou, Q.; et al. Dietary phenylalanine level could improve growth performance, glucose metabolism and insulin and mTOR signaling pathways of juvenile swimming crabs, *Portunus trituberculatus*. *Aquac. Rep.* **2022**, *27*, 101395. [CrossRef]
41. Yin, B.; Liu, H.; Tan, B.; Dong, X.; Chi, S.; Yang, Q.; Zhang, S. MHC II-PI 3 K/Akt/mTOR signaling pathway regulates intestinal immune response induced by soy glycinin in hybrid grouper: Protective effects of sodium butyrate. *Front. Immunol.* **2021**, *11*, 601665. [CrossRef]
42. Hidalgo, M.A.; Carretta, M.D.; Burgos, R.A. Long chain fatty acids as modulators of immune cells function: Contribution of FFA1 and FFA4 receptors. *Front. Physiol.* **2021**, *12*, 668330. [CrossRef] [PubMed]
43. Gutierrez, S.; Svahn, S.L.; Johansson, M.E. Effects of omega-3 fatty acids on immune cells. *Int. J. Mol. Sci.* **2019**, *20*, 5028. [CrossRef] [PubMed]

44. Lucena, M.N.; Garçon, D.P.; Fontes, C.F.L.; Fabri, L.M.; Moraes, C.M.; McNamara, J.C.; Leone, F.A. Dopamine binding directly up-regulates (Na^+, K^+)-ATPase activity in the gills of the freshwater shrimp *Macrobrachium amazonicum*. *Comp. Biochem. Physiol. Part A Mol. Integr. Physiol.* **2019**, *233*, 39–47. [CrossRef]
45. Blantz, R.C.; Satriano, J.; Gabbai, F.; Kelly, C. Biological effects of arginine metabolites. *Acta Physiol. Scand.* **2000**, *168*, 21–25. [CrossRef]
46. Akram, M. Citric acid cycle and role of its intermediates in metabolism. *Cell Biochem. Biophys.* **2014**, *68*, 475–478. [CrossRef]
47. Menzies, K.J.; Zhang, H.; Katsyuba, E.; Auwerx, J. Protein acetylation in metabolism—Metabolites and cofactors. *Nat. Rev. Endocrinol.* **2016**, *12*, 43–60. [CrossRef]
48. Zhao, Z.; YIN, Z.; WENG, S.; GUAN, H.; LI, S.; XING, K.; CHAN, S.; HE, J. Profiling of differentially expressed genes in hepatopancreas of white spot syndrome virus-resistant shrimp (*Litopenaeus vannamei*) by suppression subtractive hybridisation. *Fish Shellfish Immunol.* **2007**, *22*, 520–534. [CrossRef]
49. Hu, S.; Han, M.; Rezaei, A.; Li, D.; Wu, G.; Ma, X. L-arginine modulates glucose and lipid metabolism in obesity and diabetes. *Curr. Protein Pept. Sci.* **2017**, *18*, 599–608. [CrossRef]
50. Pizent, A. Oxidative stress-related metabolomic alterations in pregnancy: Evidence from exposure to air pollution, metals/metalloid, and tobacco smoke. *Antioxidants* **2025**, *14*, 1442. [CrossRef] [PubMed]
51. Bogaert, J.J.; Favier, J.; Ghouzzi, V.E.; Djouadi, F.; Bénit, P.; Gimenez, A.P.; Rustin, P. Succinate dehydrogenase deficiency in human. *Cell. Mol. Life Sci.* **2005**, *62*, 2317–2324.
52. Lv, L.; Xu, Z.; Zhao, M.; Gao, J.; Jiang, R.; Wang, Q.; Shi, X. Mannose inhibits *Plasmodium parasite* growth and cerebral malaria development via regulation of host immune responses. *Front. Immunol.* **2022**, *13*, 859228. [CrossRef] [PubMed]
53. Obrosova, I.G.; Pacher, P.; Szab, C.; Zsengeller, Z.; Hirooka, H.; Stevens, M.J.; Yorek, M.A. Aldose reductase inhibition counteracts oxidative-nitrosative stress and poly (ADP-ribose) polymerase activation in tissue sites for diabetes complications. *Diabetes* **2005**, *54*, 234–242. [CrossRef] [PubMed]
54. Li, H.; Meng, Q.; Wang, W.; Mo, D.; Dang, W.; Lu, H. Gut microbial composition and liver metabolite changes induced by ammonia stress in juveniles of an invasive freshwater Turtle. *Biology* **2022**, *11*, 1315. [CrossRef] [PubMed]

Disclaimer/Publisher's Note: The statements, opinions and data contained in all publications are solely those of the individual author(s) and contributor(s) and not of MDPI and/or the editor(s). MDPI and/or the editor(s) disclaim responsibility for any injury to people or property resulting from any ideas, methods, instructions or products referred to in the content.